Frontiers in Bioscience Landmark

Front. Biosci. (Landmark Ed) **2026**; 31(8): 53953
https://doi.org/10.31083/FBL53953

Original Research

PF-127 Hydrogel-Delivered hUCMSC-Exosomes Attenuate Endometrial Injury by Inhibiting Epithelial-Mesenchymal Transition

Liwei Bao[1,†], Li Li[2,†], Shengbin Tang[3], Yezi Tang[3], Zihan Wang[1], Jiaxi Tan[1], Huihui Zhang[1], Rushi Liu[1,*], Xia Zhang[1,*]

[1]School of Medical Technology and Translational Medicine, Hunan Normal University, 410000 Changsha, Hunan, China
[2]Hunan Provincial Key Laboratory of Regional Hereditary Birth Defects Prevention and Control, Changsha Hospital for Maternal & Child Health Care Affiliated to Hunan Normal University, 410000 Changsha, Hunan, China
[3]Center for Cell and Regenerative Medicine, Hunan Shengbao Biotechnology Co., Ltd., 410000 Changsha, Hunan, China
*Correspondence: liurushi@hunnu.edu.cn (Rushi Liu); zx717@hunnu.edu.cn (Xia Zhang)
[†]These authors contributed equally.
Academic Editor: Francesca Diomede
Submitted: 17 May 2026 Revised: 6 July 2026 Accepted: 15 July 2026 Published: 21 August 2026

Abstract

Background: Endometrial injury, often resulting from iatrogenic procedures or infections, can lead to fibrosis, adhesions, and infertility. Current therapies are inadequate for reversing fibrosis or restoring normal function. Mesenchymal stem cell-derived exosomes (MSC-exos) present therapeutic potential; however, their rapid clearance poses a challenge. The purpose of this study was to develop a thermosensitive Pluronic F-127 (PF-127) hydrogel for sustained intrauterine delivery of human umbilical cord MSC-derived exosomes (PF-127-hUCMSC-exos) and to evaluate its efficacy and underlying mechanisms in a rat model of ethanol-induced endometrial injury. **Methods:** A thermosensitive PF-127 hydrogel loaded with hUCMSC-exos was developed. Its retention and therapeutic effects were evaluated in a rat model of ethanol-induced endometrial injury. Comparisons were made among control, model, hydrogel treatment alone, and PF-127-hUCMSC-exos treatment. Mechanistic assessments included histological analysis, collagen deposition measurement, fertility testing, expression analysis of epithelial-mesenchymal transition (EMT) markers (E-cadherin, vimentin, β-catenin), transcriptomic analysis of exosome-treated primary rat endometrial stromal cells, and measurement of early growth response 2 (EGR2) mRNA and protein levels. **Results:** PF-127-hUCMSC-exos were detectable in the uterine cavity up to day 12, and this treatment significantly improved endometrial morphology, increased thickness and gland number, reduced collagen deposition, and partially restored fertility. Mechanistically, exosomes inhibited EMT by upregulating E-cadherin and downregulating vimentin and β-catenin. RNA-seq of exosome-treated rESCs identified 1173 differentially expressed genes, with enrichment in EMT-related pathways. EGR2, a pro-fibrotic transcription factor, was significantly downregulated at both mRNA and protein levels. EGR2 overexpression promoted cell migration, which was reversed by exosome treatment. **Conclusions:** PF-127-hUCMSC-exos hydrogel effectively repairs endometrial injury and restores fertility by inhibiting EMT, potentially via EGR2 downregulation. This cell-free strategy offers a promising approach for endometrial regeneration.

Keywords: mesenchymal stem cell; exosomes; endometrium injuries; epithelial-mesenchymal transition; Pluronic F-127

1. Introduction

The integrity of the endometrial basal layer is a physiological prerequisite for the regulation of the menstrual cycle and for embryo implantation. However, various iatrogenic procedures, including repeated intrauterine surgeries, as well as infections and inflammatory diseases, can damage the endometrial basal layer. This damage leads to impaired endometrial regeneration, abnormal fibrosis, and intrauterine adhesions. These conditions are significant contributors to female infertility, recurrent implantation failure, and pregnancy loss. Current treatments, such as hysteroscopic adhesiolysis combined with hormonal therapy, only partially restore the anatomical structure and do not effectively reverse fibrosis or recover functionality, resulting in high recurrence rates [1,2,3]. Therefore, novel regenerative strategies that can inhibit fibrosis and restore endometrial homeostasis are urgently needed.

In recent years, cell therapy, particularly mesenchymal stem cell (MSC) transplantation, has emerged as a prominent area of research. MSCs can be isolated from various tissues and administered via tail vein or intrauterine injection to promote endometrial thickening and gland and blood vessel formation and to enhance embryo receptivity [4,5]. However, the use of live cells carries risks of immune rejection and embolism. Moreover, large-scale cultivation may even diminish the therapeutic properties of MSCs [6]. The exosomes secreted from MSCs (MSC-exos), which mimic paracrine effects by transporting miRNAs and proteins to promote angiogenesis and suppress inflammatory fibrosis, have been validated in rat models of ethanol-induced or mechanical endometrial injury [7,8,9]. Nevertheless, exosomes are rapidly cleared after intrauterine administration, resulting in low delivery efficiency. Pluronic F-127 (PF-127) thermosensitive hydrogel, known

Copyright: © 2026 The Author(s). Published by IMR Press.
This is an open access article under the CC BY 4.0 license.

Publisher's Note: IMR Press stays neutral with regard to jurisdictional claims in published maps and institutional affiliations.

for its biocompatibility and injectability, can slowly release nanovesicles after gelation, thereby prolonging retention and providing a viable carrier for cell-free repair [10,11]. Current research is focused on PF-127 hydrogel loaded with stem cells or exosomes to promote wound healing [12,13], while studies on its application in the noninvasive treatment of endometrial injury using MSC-exos are limited.

A key mechanism through which MSCs and MSC-exos facilitate tissue repair is the alleviation of fibrosis in damaged tissues [14]. Epithelial–mesenchymal transition (EMT) is often activated during inflammatory responses, wound healing, and fibrotic processes. In instances of mild injury, EMT promotes the transformation of epithelial cells into myofibroblasts, thereby enhancing tissue repair. However, under chronic inflammatory conditions, the abnormal and sustained activation of EMT results in excessive accumulation of myofibroblasts and extracellular matrix deposition, ultimately disrupting the structure and function of parenchymal organs [15]. The regulation of EMT involves multiple signaling pathways, with the transforming growth factor-β (TGF-β) family serving as the primary inducer [16,17]. Additionally, the Notch signaling pathway [18,19], the canonical Wnt pathway, and various inflammatory cytokines collectively contribute to the initiation and maintenance of EMT [20,21]. Studies have demonstrated that MSCs can inhibit the EMT process and alleviate fibrosis by modulating signaling pathways such as Wnt/β-catenin and TGF-β/Smad [22]. Furthermore, the reversal effect of MSC-exos on EMT is linked to miRNA delivery and transcriptional regulation. Specifically, miR-23a-3p and miR-182-5p carried by MSC-exos can inhibit Ikbkb, thereby downregulating the NF-κB and Hedgehog signaling pathways and thus mitigating LPS-induced pulmonary fibrosis [23]. Similarly, miR-466f-3p derived from mouse MSC-exos can target c-MET and inhibit the AKT/GSK3β pathway, thereby reversing the EMT process in radiation-induced lung injury [24]. These findings indicate that MSCs and their exosomes play crucial roles in suppressing fibrosis and promoting tissue regeneration by regulating EMT through multiple pathways and targets.

In this study, we prepared a PF-127 hydrogel for the sustained release of human umbilical cord MSC-derived exosomes (PF-127-hUCMSC-exos) and investigated its therapeutic potential for endometrial injury, its effects on fertility function, and its underlying mechanisms. We found that hUCMSC-exos improved endometrial fibrosis in injured rats by inhibiting EMT, potentially through the downregulation of the EMT-related molecule EGR2, thereby providing a translatable new approach for the clinical repair of moderate to severe endometrial damage.

2. Materials and Methods

2.1 Isolation of hUCMSC-Exosomes

hUCMSC-exos used in the experiment were isolated by ultracentrifugation from the cell culture supernatant provided by Hunan Shengbao Biotechnology Co., Ltd. The supernatant from hUCMSCs cultured through passages 3 to 5 was collected. Following the removal of cells and debris by differential centrifugation at 300, 2000, and 10,000 ×g, the exosomes were pelleted by ultracentrifugation at 110,000 ×g for 70 minutes at 4 °C. The resulting exosome pellet was then resuspended in sterile PBS, aliquoted, and stored at –80 °C.

2.2 Preparation of PF-127 Hydrogel

PF-127 powder (P2443-250G, Sigma, Missouri, USA) was added to pre-cooled PBS buffer at 4 °C under sterile conditions to achieve the desired concentration (e.g., 30%, w/v). The mixture was placed on a magnetic stirrer at 4 °C and stirred at low speed overnight until the powder was completely dissolved, resulting in a clear, transparent pre-gel solution. This solution remains liquid at low temperatures but transitions rapidly to a gel state at body temperature. The final concentration of the hydrogel used for injection was 25%, and the loading concentration of hUCMSC-exos in the PF-127 hydrogel was 20 μg/mL, which corresponds to 2 μg of exosomes per rat in a 100 μL injection volume.

2.3 Cell Culture

Rat renal epithelial cells (NRK-52E) were purchased from the American Type Culture Collection (CRL-1571) and maintained in Dulbecco's modified Eagle's medium (30030, Gibco, Massachusetts, USA) supplemented with 10% fetal bovine serum (A5669701, Gibco) and 100 U penicillin/streptomycin (15140122, Gibco) at 37 °C in a 5% CO_2 incubator. All cell lines were validated by STR profiling and tested negative for mycoplasma.

To generate primary rat endometrial stromal cells (rESCs), female SD rats were subcutaneously injected with 17β-estradiol (3.5 mg/kg) for 3 consecutive days to synchronize their estrus. After euthanasia, uteri were excised, washed three times with HBSS, and minced into 0.5–1 mm^3 pieces. The tissues were digested with 0.8 mg/mL collagenase I at 37 °C for 60 min, terminated with DMEM/F12 (11320033, Gibco) supplemented with 10% FBS, filtered through a 400-mesh sieve, and centrifuged to collect the cells, and cultured at 37 °C in a 5% CO_2 incubator. Primary culture was performed until passage 3, with identification based on morphology and vimentin expression.

2.4 EMT Induction and Transwell Assay

The test cells, such as NRK-52E cells or rESCs, were seeded into 6-well plates and divided into three groups. Upon reaching 90% confluence, the model group was treated with 50 ng/mL TGF-β, while the treatment group received the same concentration of TGF-β (50 ng/mL) along with 1 μg/mL exosomes. Cells were harvested for protein or RNA extraction 24 hours post-treatment. For transwell assay, cells were resuspended in serum-free medium

and seeded in the upper chamber of the Transwell insert. The model group was treated with 50 ng/mL TGF-β, while thetreatment group received the same dose of TGF-β along with 1 μg/mL exosomes. Complete medium containing 10% FBS was added to the lower chamber as a chemoattractant. The culture plate was placed in a 37 °C incubator with 5% CO_2 for 24 hours. The chamber was subsequently removed, and the cells that migrated to the membrane of the lower chamber were fixed with 4% paraformaldehyde and stained with 0.1% crystal violet. Multiple random fields of view were then photographed and counted under a microscope (Carl Zeiss AG, Baden-Württemberg, Germany), followed by statistical analysis of the cell migration count.

2.5 In Vivo Experimental Design

All animal protocols were approved by the Ethics Committee of Hunan Normal University (permit number: 2022431; approval date: October 2022). The study was carried out in accordance with the ARRIVE guidelines. Eight-week-old female SD rats (Beijing Vital River) were synchronized using vaginal smears, and surgery was performed during estrus. Animals with body weight of 180–220 g and normal estrous cycles were included, excluding those with preoperative illness, intraoperative complications, or >20% postoperative weight loss. Following intraperitoneal (i.p.) injection of 1.5% sodium pentobarbital at 70 mg/kg, a midline laparotomy was conducted to expose both uterine horns. A microsyringe (1 mL) was used to infuse absolute ethanol (100 μL) into each lumen upward from the Y-shaped bifurcation of the rat uterus for five minutes to induce endometrial injury, followed by three saline washes. The sham operation group without ethanol injury served as the control group (n = 8). The injured animals (n = 24) were then randomly assigned to one of three groups: (1) injury-only (Model), (2) PF-127 hydrogel vehicle (100 μL), or (3) PF-127-hUCMSC-exos (100 μL). After *in situ* gelation, the uterus was repositioned, and the abdomen was closed. Standard postoperative care was provided. At the third estrus postinjury (about 14 days), the rats were sacrificed by CO_2 euthanasia (10 L progressive chamber, 5 L/min for 7 min, with an additional 1 min after respiratory arrest), and the uteri were fixed in 4% paraformaldehyde for hematoxylin and eosin (H&E) and Masson's trichrome staining. For fertility assessment, only the left uterine horn was injured using the same procedure, while the right horn remained untreated as an internal control (n = 5 per group). On day 14 post-intervention, rats in the fertility assessment groups were paired 1:1 with proven fertile males. The presence of a vaginal plug and a sperm-positive smear the following morning was designated as gestation day 0. On day 18 of pregnancy, the dams were euthanized using the same CO_2 method, the uterine horns were opened, and implantation sites were counted to evaluate reproductive recovery.

2.6 Exosome Labeling and In Vivo Tracking

hUCMSC-exosomes were labeled with PKH26 red fluorescent dye (123452207, Sigma, MINI26-1KT, USA) following the manufacturer's instructions. After a rat endometrial injury model was established, a PF-127 hydrogel loaded with PKH26-labeled exosomes was injected into the uterine cavity. The animals were sacrificed at 0, 4, 6, 8, 10, and 12 days postinjection, after which the uterine tissues were collected. The overall fluorescence signals from the uterine tissues were captured using a small-animal *in vivo* imaging system (PerkinElmer, Massachusetts, USA) to semiquantitatively analyze the retention time of the exosomes at the injury site. Moreover, portions of fresh uterine tissue were embedded in optimal cutting temperature (OCT) compound and rapidly frozen in liquid nitrogen. Frozen sections were prepared, and after Hoechst 33342 nuclear staining was performed, the distribution and localization of the exosomes in the uterine tissue sections were observed using a laser confocal microscope (Leica, Hesse, Germany).

2.7 Histological Staining

Uterine tissues were fixed in 4% paraformaldehyde, dehydrated through a graded series of ethanol, cleared in xylene, embedded in paraffin, and sectioned at 4 μm. For H&E staining, the sections were sequentially dewaxed in xylene, hydrated through graded ethanol, stained with hematoxylin, differentiated in hydrochloric acid–alcohol, blued in running water, counterstained with eosin, dehydrated, cleared, and mounted with neutral resin. For Masson's trichrome staining, dewaxed and hydrated sections were sequentially stained with Weigert's iron hematoxylin for nuclei and Ponceau-acid fuchsin for cytoplasm and muscle fibers, differentiated in a phosphomolybdic acid solution, stained with aniline blue for collagen fibers, and subsequently treated with a weak acid solution, dehydrated, cleared, and mounted. All stained sections were observed under an optical microscope, and images were captured. Quantitative analysis of endometrial thickness relative to total uterine wall thickness, gland number, and collagen fiber area percentage was performed using ImageJ software (ImageJ 1.54p).

2.8 Immunofluorescence

Frozen sections of OCT-embedded uterine tissues were rewarmed to room temperature and rinsed with PBS to eliminate the embedding medium. The sections were then fixed in 4% paraformaldehyde (Biosharp, Beijing, China) for 10 minutes, followed by three washes with PBS. The sections were subsequently blocked using a solution containing 5% bovine serumalbumin (ST023, Beyotime, Shanghai, China) and 0.3% Triton X-100 (ST1723, Beyotime) at room temperature for 1 hour. After the blocking solution was removed, a diluted primary antibody including anti-vimentin (A19607, Abclonal, Wuhan, China,

1:200), anti-E-cadherin (14472T, Cell Signaling Technology, USA, 1:100) was added, and the samples were incubated overnight at 4 °C. The following day, the primary antibody was removed by washing with PBS, and species-specific fluorescently labeled secondary antibodies, FITC (AS011, Abclonal, 1:100), Cy3 (AS008, Abclonal, 1:100) were added, followed by incubation at room temperature in the dark for 1 hour. After an additional PBS wash, the nuclei were counterstained with Hoechst 33342 (C1053, Beyotime). Finally, anti-fade mounting medium was applied to seal the sections. Fluorescence images of specific target proteins were observed and captured using a laser confocal microscope (Leica).

2.9 RTqPCR

Total RNA was extracted from cells or ground uterine tissues using TRIzol reagent (Invitrogen), and its concentration and purity were measured with a microspectrophotometer (Thermo Fisher NanoDROP One, Massachusetts, USA). An equal amount of total RNA was used to synthesize first-strand cDNA according to the instructions provided with the reverse transcription kit (RR036A, TAKARA, Shiga, Japan). qPCR was performed on a real-time fluorescence quantitative PCR instrument using a SYBR Green premix system (RR4230A, TAKARA). The reaction program consisted of predenaturation at 95 °C for 30 seconds, followed by 40 cycles of denaturation at 95 °C for 5 seconds and annealing/extension at 60 °C for 30 seconds. All samples were run in triplicate, with glyceraldehyde-3-phosphate dehydrogenase (GAPDH) used as the reference gene. The relative expression levels of target genes were calculated using the $2^{-\Delta\Delta Ct}$ method.

2.10 Western Blot

Total protein was extracted from cells or tissues using RIPA lysis buffer supplemented with protease inhibitors, and the protein concentration was determined via the BCA method. Equal amounts of protein samples were separated using SDS–PAGE, after which the proteins were transferred to PVDF membranes by the wet transfer method. After blocking with 5% skim milk in TBST at room temperature for 1 hour, the membranes were incubated overnight at 4 °C with diluted primary antibodies, including CD63 (25682-1-AP, Proteintech, Wuhan, China), TSG101 (28283-1-AP, Proteintech), calnexin (10427-2-AP, Proteintech), vimentin (A19607, ABclonal, Wuhan, China), β-catenin (A20221, ABclonal), β-actin(AF5003, Beyotime Shanghai, China), and EGR2 (A3219, ABclonal). Following three washes with TBST, the membranes were incubated with the corresponding horseradish peroxidase-conjugated secondary antibodies at room temperature for 1 hour. After thorough washing, the membranes were treated with enhanced chemiluminescence (ECL) detection reagents, and signals were captured using a chemiluminescence imaging system (Tanon, Shanghai, China).

2.11 RNA Sequencing

The rESCs were treated with exosomes (with PBS as the control) at a final concentration of 0.5 μg/mL for 24 hours. Subsequently, total RNA was isolated using TRIzol reagent, and mRNA was enriched using oligo(dT) magnetic beads and fragmented. The cDNA library was amplified by PCR with appropriate cycling parameters, quality controlled, and sequenced on the DNBSEQ platform (BGI). Raw sequencing data were processed using SOAPnuke (v2.2.1, Shenzhen, China) for quality filtering. Subsequent bioinformatics analysis, visualization, and multiomics data mining were performed using the Dr. Tom integrated analysis platform. The differentially expressed genes (DEGs) were defined as those whose $|\log_2 \text{fold change}|$ was ≥ 1.0 and whose FDR was <0.05.

2.12 Statistical Analyses

Data from three independent experiments were analyzed using GraphPad Prism 10.0 software (San Diego, California, USA) and are shown as the mean ± SEM. Statistical multigroup comparisons were performed by ANOVA, followed by a Student–Newman–Keuls post hoc test. Two-tailed unpaired Student's t tests were used to compare two groups. *p* values less than 0.05 were considered to indicate statistical significance.

3. Results

3.1 Characterization of PF-127-hUCMSC-Exos

Exosomes were isolated using ultracentrifugation, and transmission electron microscopy revealed that the exosomes exhibited a round vesicle-like structure (Fig. 1A). Dynamic light scattering analysis revealed that the particle size distribution ranged from 100 to 1000 nm (Fig. 1B). Western blot analysis of exosomal surface protein markers revealed that both human umbilical cord mesenchymal stem cells and exosomes expressed CD63 and TSG101 (Fig. 1C), whereas calnexin was expressed only in human umbilical cord mesenchymal stem cells and not in exosomes. The quantified exosomes were incorporated into the PF-127 hydrogel, which remained in a liquid state at 4 °C and transformed into a solid state at 37 °C (Fig. 1D). This hydrogel exhibits temperature sensitivity, injectability, and minimal flow after solidification.

3.2 In Vivo and In Vitro Tracing of PF-127-hUCMSC-Exos

We labeled exosomes with the red fluorescent PKH26 dye and traced them to renal tubular epithelial cells. Red exosome fluorescence signals were detected in the cells 6 hours after the direct addition of exosomes, with the fluorescence signals gradually intensifying over time. However, almost no exosome fluorescence signals were observed in the PF-127-loaded exosome group at the 6-hour time point (Fig. 2A). These findings suggest that exosomes can be taken up by cells and that PF-127 hydrogel-loaded exosomes can achieve sustained release.

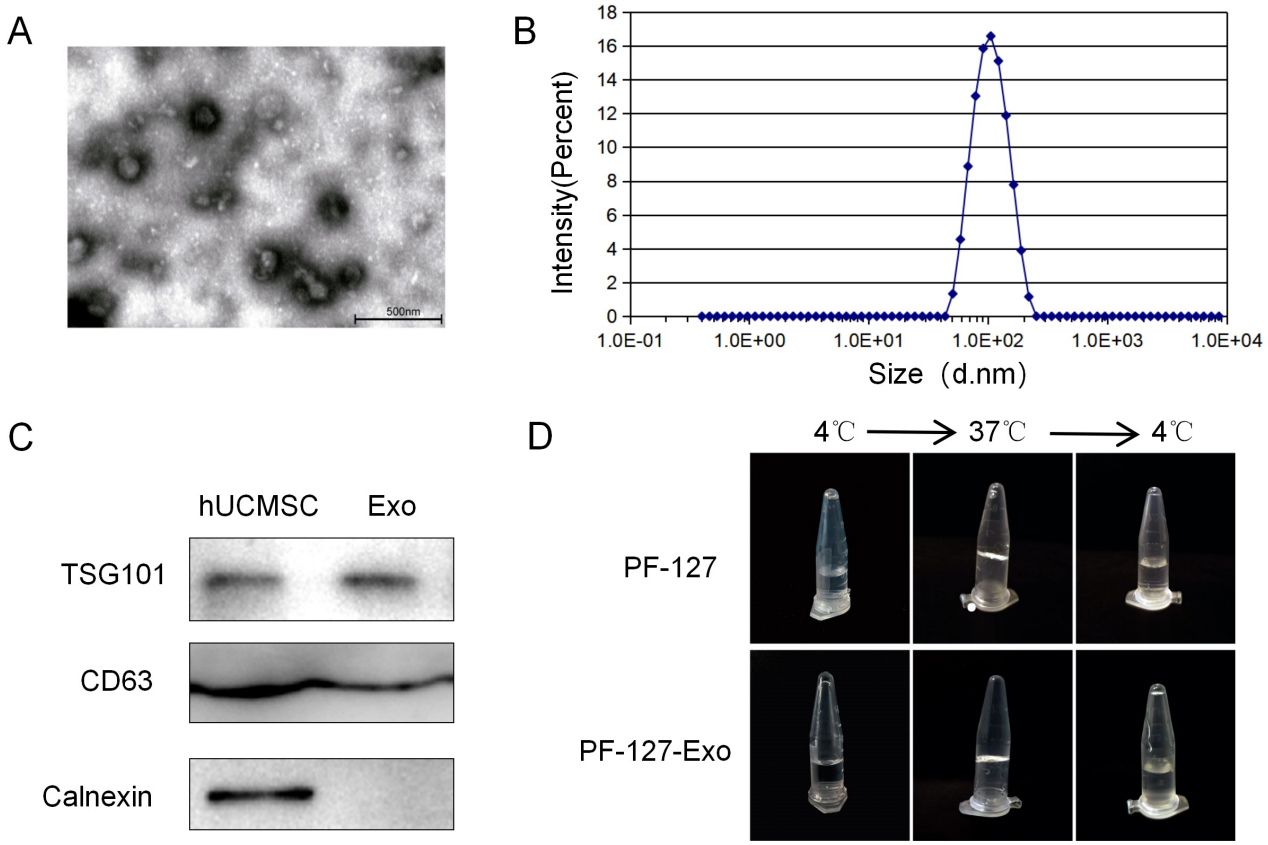

Fig. 1. Characterisation of hUCMSC-Exo and preparation of thermosensitive Pluronic F-127 (PF-127) hydrogel. (A) Representative transmission electron microscopy (TEM) image of isolated exosomes. Scale bar = 500 nm. (B) Size distribution profile of exosomes as determined by dynamic light scattering (DLS). (C) Western blot analysis of exosomal and cellular markers, including TSG101, CD63 and Calnexin. (D) Photographs of the PF-127 hydrogel at 4 °C and 37 °C, demonstrating the sol-gel phase transition (liquid at 4 °C, gel at 37 °C).

We subsequently conducted *in vivo* exosome tracing in rats. The results demonstrated that exosome fluorescence signals were detected in the uterine cavity on day 0 post-injection and persisted until day 12 (Fig. 2B,C). This indicates that PF-127 hydrogel-loaded exosomes can be slowly released and preserved long term in the rat uterine cavity. Additionally, we obtained frozen sections of rat uterine tissue and collected fluorescence images using confocal laser scanning microscopy. Weak exosome fluorescence signals were observed in the uterine tissue on day 0; these signals initially increased but then decreased over time, which is consistent with previous results (Fig. 2D). These findings demonstrate that PF-127 loaded exosomes achieve sustained release, and can be taken up by uterine tissue to exert sustained therapeutic effects.

3.3 PF-127-hUCMSC-Exos Can Improve the Function of Damaged Uterus

To investigate the effects of exosomes on endometrial injury, we established an endometrial injury model by injecting absolute ethanol into the uterine cavity of rats during the estrus phase, followed by treatment with PF-127-hUCMSC-exos. After three estrus cycles (about 14 days) of treatment, uterine tissues were collected for analysis (Fig. 3A). H&E staining revealed a significant reduction in endometrial thickness and a decrease in the number of glands in both the model group and the PF-127 hydrogel group. In contrast, the PF-127-hUCMSC-exos group exhibited a marked increase in endometrial thickness and restoration of gland numbers (Fig. 3B,C,D). Masson staining further revealed that the fibrotic area of the endometrium and collagen fiber deposition significantly increased in both the model and PF-127 hydrogel groups, whereas the exosome-treated group demonstrated a significant reduction in collagen fiber area and alleviation of fibrosis (Fig. 3B,E).

We subsequently evaluated the fertility of the rats. Uterine injury modeling and PF-127 hydrogel exosome therapy were conducted during the estrus phase. After 14 days of treatment, female rats were co-housed with male rats. Vaginal secretions were collected the following morning, and the presence of sperm observed under microscopy was recorded as gestational day 0. Uteri were harvested on gestational day 18, and the number of implantation sites was counted (Fig. 4A). The results indicated that rats with

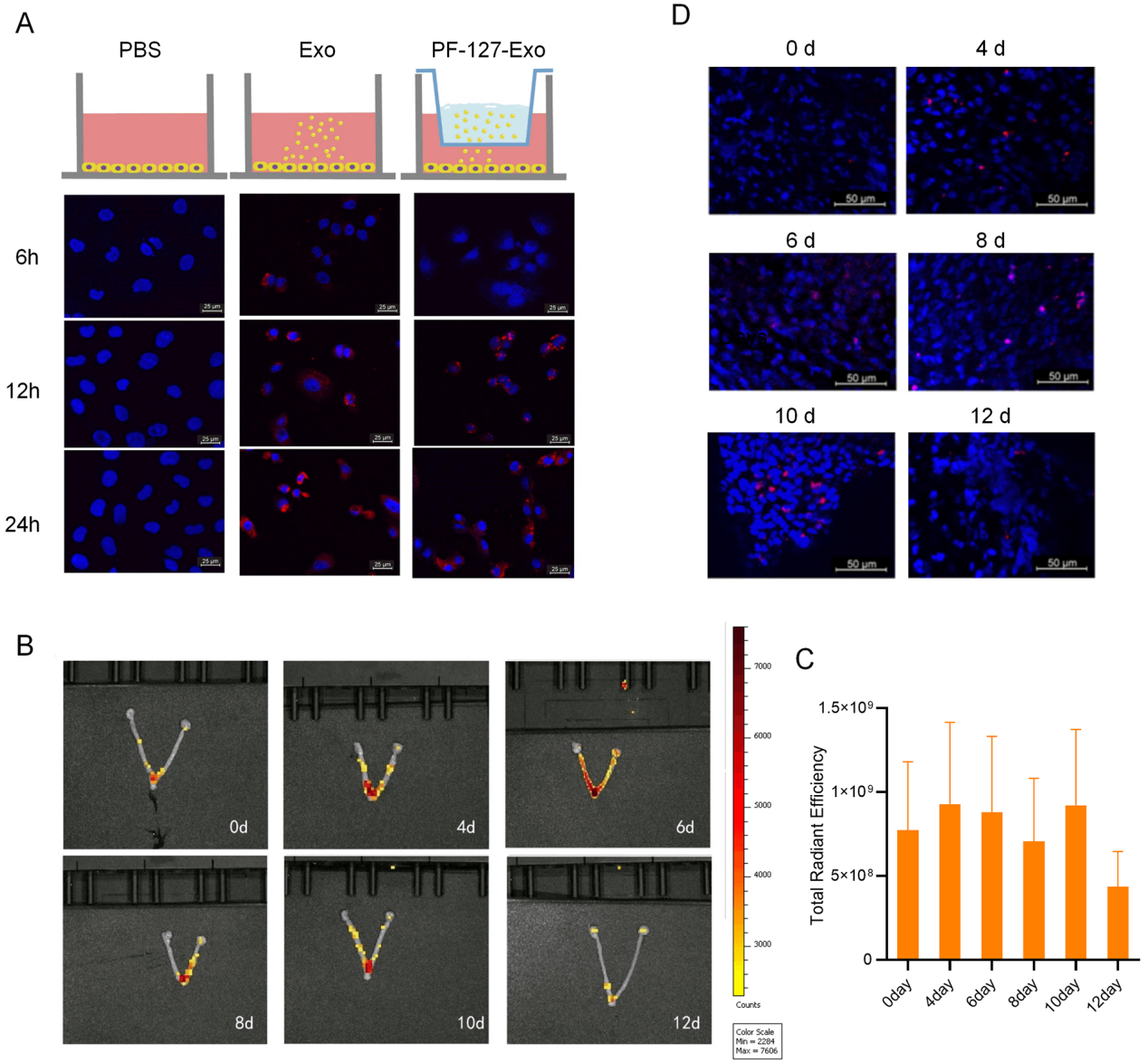

Fig. 2. ***In vitro*** **and** ***in vivo*** **tracking of PKH26-labelled exosomes (PKH26-Exo).** (A) Representative immunofluorescence images show PKH26 (red) signal in cells treated with PKH26-Exo with or without PF-127 hydrogel encapsulation. Nuclei were stained with Hoechst 33342 (blue). Scale bar = 25 μm. (B) The fluorescence imaging of the rat uterine cavity following intrauterine injection of PF-127-PKH26-Exo hydrogel. Images were acquired at the indicated time points (days 0, 4, 6, 8, 10, and 12) using a small animal *in vivo* imaging system. (C) Quantification of the fluorescence intensity in the uterine cavity (n = 3) from the images shown in (B) over the 12-day period. (D) Representative fluorescence images of uterine tissues harvested at the indicated time points, demonstrating the retention and distribution of PKH26-Exo. Nuclei were stained with Hoechst 33342 (blue). Scale bar = 50 μm.

left uterine injuries induced by absolute ethanol and treated with PF-127 hydrogel failed to achieve successful pregnancy, whereas those treated with exosomes successfully conceived (Fig. 4B,C).

3.4 hUCMSC-Exos Inhibit the EMT Process

To elucidate the potential mechanisms through which hUCMSC-exos promote endometrial injury repair, we examined its effects on cell migration. First, Transwell assays were conducted to assess the effects of exosomes on the migration capabilities of rat renal epithelial cells (NRK-52E) and primary ESCs. The findings revealed a significant decrease in the number of migrating cells in both cell types after exosome intervention (Fig. 5A,B). Based on these observations, we speculate that the reparative effect of hUCMSC-exos on the endometrium may be linked to the regulation of the EMT process.

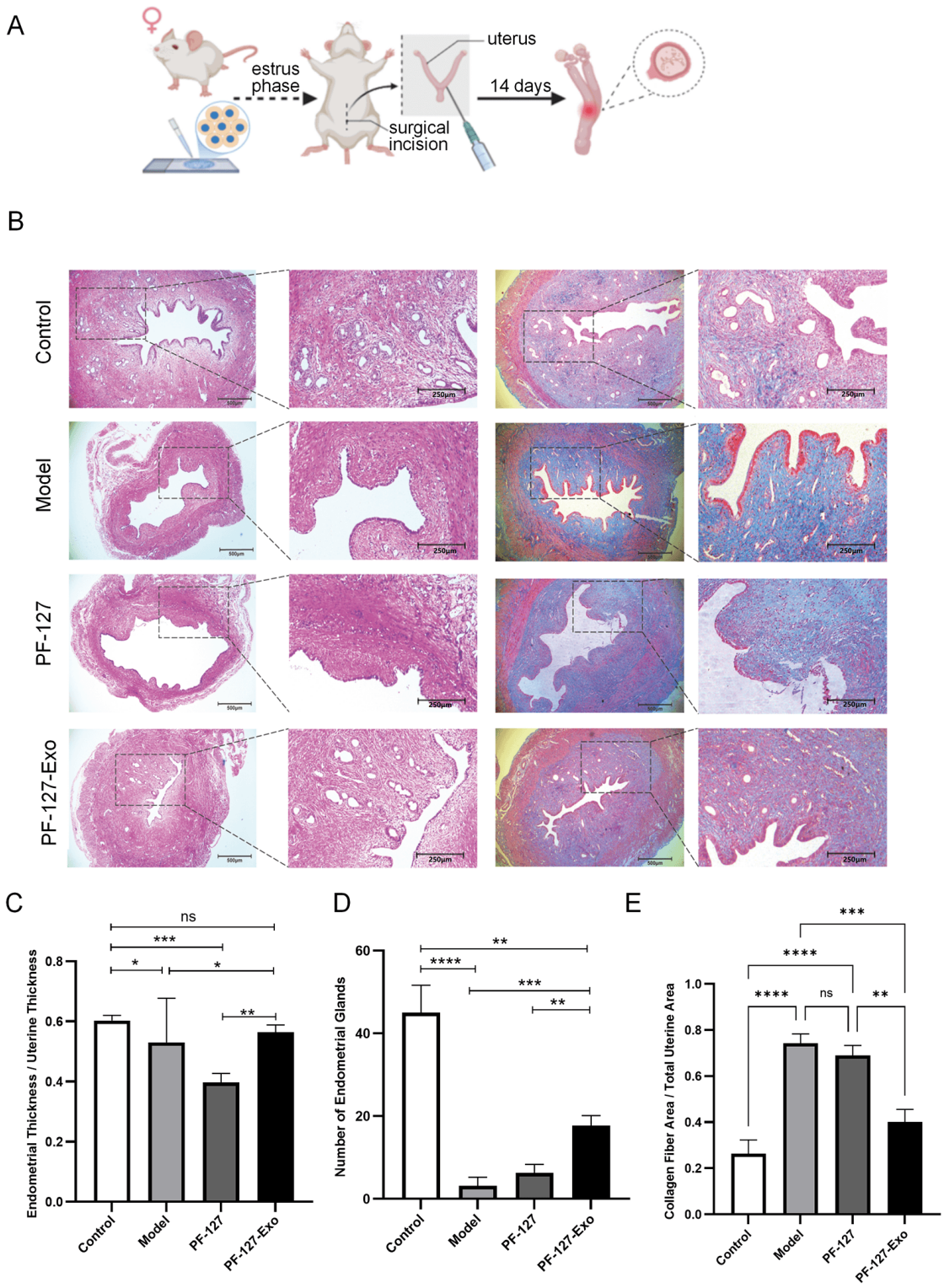

Fig. 3. Therapeutic efficacy of PF-127-hUCMSC-Exo in a rat model of absolute ethanol-induced uterine injury. (A) Schematic diagram of the experimental timeline for establishing the uterine injury model and subsequent PF-127-Exo treatment. (B) Representative images of H&E staining showing uterine tissue histoarchitecture and Masson's trichrome staining indicating collagen deposition (blue) in fibrotic areas. Scale bars = 500 and 250 μm. (C–E) Quantitative analysis of histological parameters. (C) Endometrial thickness relative to total uterine wall thickness. (D) Gland count per uterine cross-section. (E) Fibrotic area percentage relative to total tissue area. Data are presented as mean ± SEM. *$p < 0.05$, **$p < 0.01$, ***$p < 0.001$, ****$p < 0.0001$, ns: no significance.

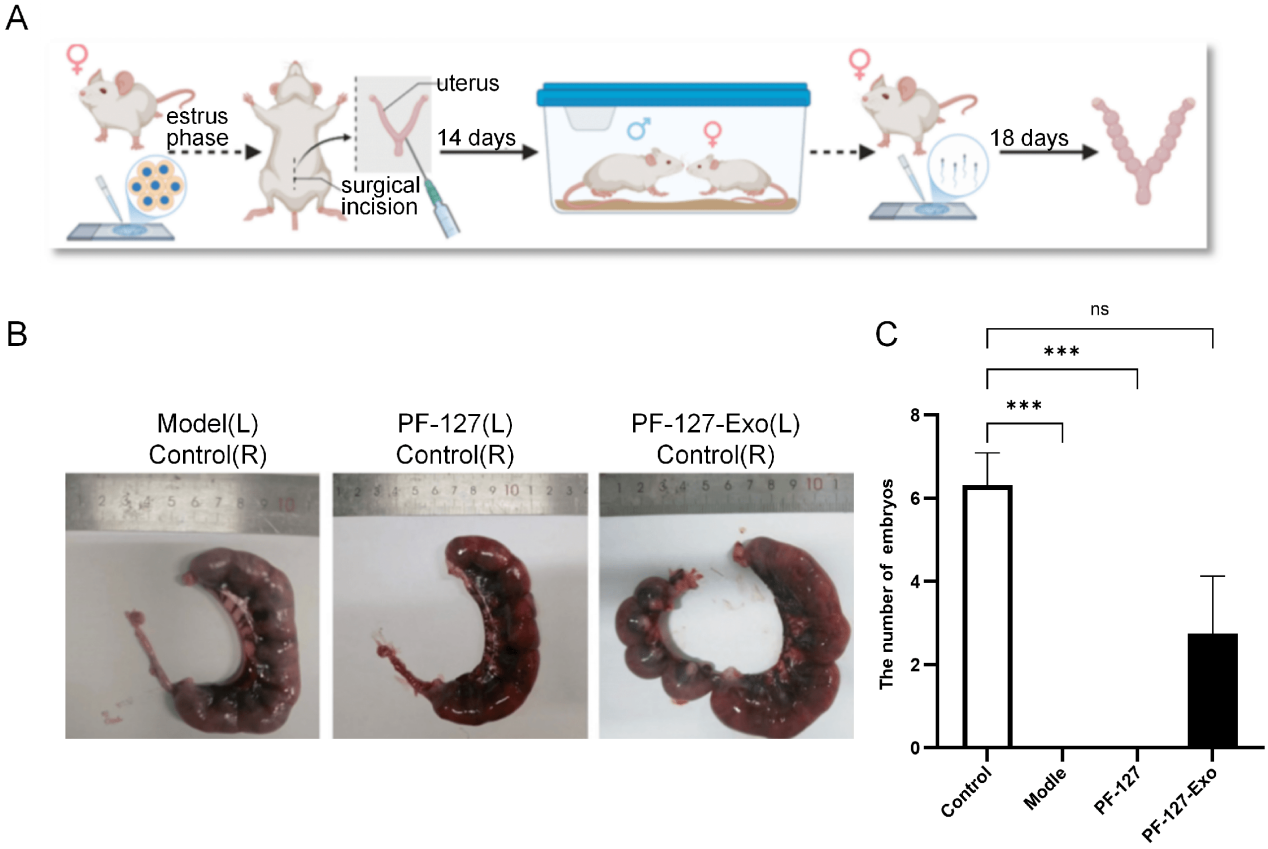

Fig. 4. Restoration of fertility in injured rats following PF-127-hUCMSC-Exo treatment. (A) Schematic of the mating experiment to assess fertility recovery after uterine injury and treatment. (B) Representative photographs of uteri excised at embryonic day 18 post-mating. Embryos are visible in the control and PF-127-hUCMSC-Exo-treated groups, but absent in the model and PF-127-only groups. (C) Statistical comparison of the number of implanted sites per uterus across different groups (n = 5/group). Data are presented as mean ± SEM. ***$p < 0.001$, ns: no significance.

To validate this hypothesis, Western blot and qPCR were used to detect changes in the expression of core EMT markers. The results demonstrated that, at the mRNA levels, the expression of N-cadherin and β-catenin was significantly downregulated, while E-cadherin was markedly upregulated in the exosome intervention group. At the protein level, the expression of vimentin and β-catenin was also significantly decreased. These results suggest that exosomes can inhibit the EMT process (Fig. 5C,D). Additionally, the expression of EMT marker proteins was evaluated by immunofluorescence staining of frozen sections. Compared with that in the sham surgery group, the fluorescence intensity of endometrial E-cadherin was significantly lower in both the model group and the PF-127 group, whereas vimentin expression was higher. After treatment with PF-127-hUCMSC-exos, E-cadherin expression was significantly restored, and the vimentin fluorescence signal was markedly diminished (Fig. 5E). Collectively, these results indicate that hUCMSC-exos promote structural repair of the endometrium following injury by inhibiting the EMT process and maintaining the epithelial phenotype.

3.5 Transcriptomic Analysis of Differentially Expressed Genes in ESCs Cocultured With hUCMSC-Exos

To investigate the transcriptomic characteristics of primary ESCs following hUCMSC-exos intervention, we employed high-throughput RNA sequencing. The results revealed 1173 transcripts whose expression was significantly altered, including 527 upregulated genes and 646 downregulated genes. Gene Ontology (GO) analysis revealed significant enrichment in biological processes related to "cell migration", "endothelial cell migration", and "epithelial to mesenchymal transition (EMT)" (Fig. 6A). KEGG pathway classification further revealed that the DEGs were enriched primarily in categories such as "TGF-β signaling pathway", "Wnt signaling pathway", and "Notch signaling pathway", which are closely related to EMT (Fig. 6B). Based on expression magnitude and functional relevance, we identified key candidate genes, such as NOG, NPR3, MAP3K7C1, and EGR2. The results of quantitative real-time PCR (qPCR) validation were highly consistent with the sequencing data: NOG and NPR3 mRNA expression was significantly upregulated ($p < 0.05$), whereas

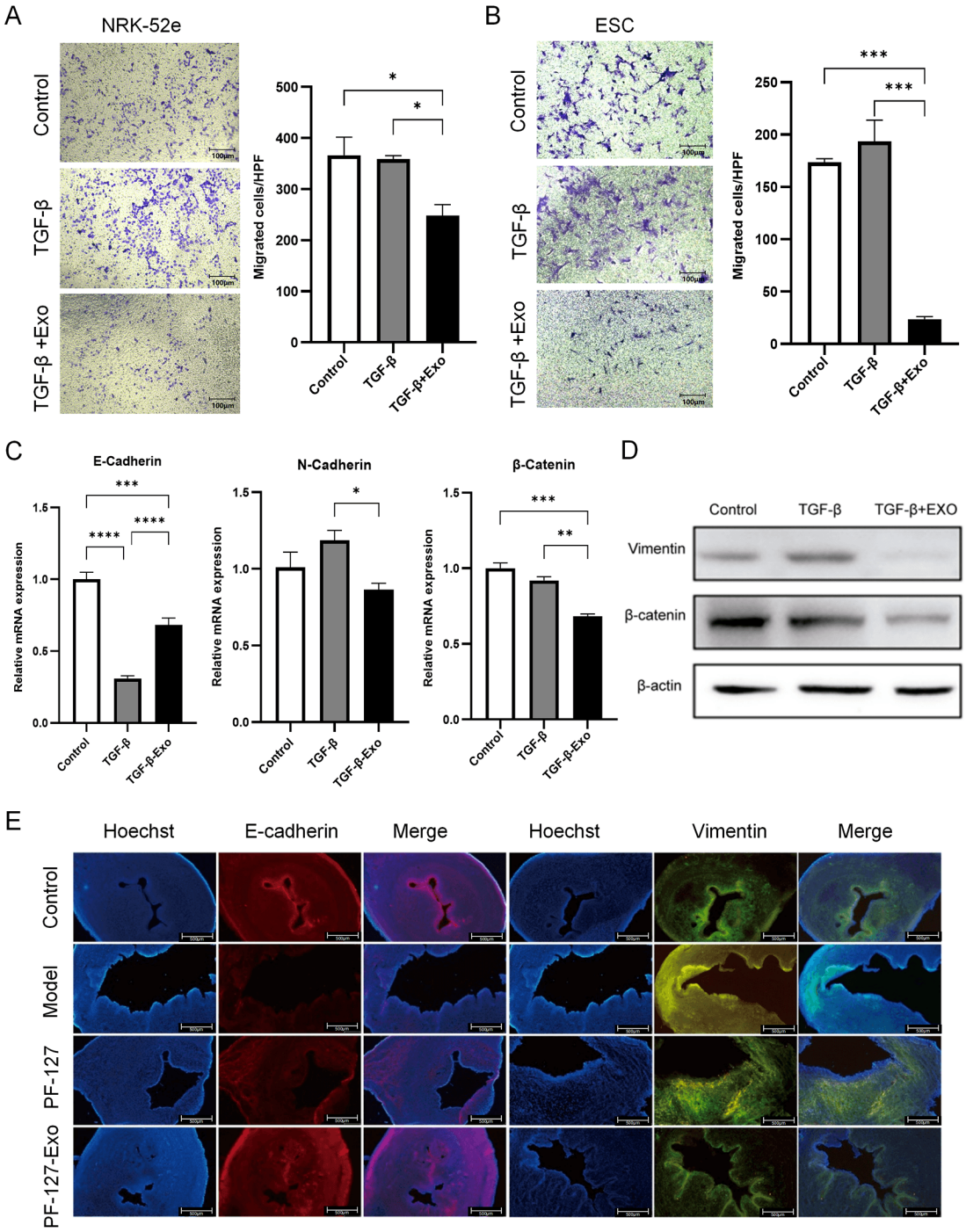

Fig. 5. hUCMSC-Exosomes inhibit EMT *in vitro* and *in vivo*. (A,B) (Left) Representative images of Transwell migration assays (crystal violet staining) for (A) NRK-52E and (B) ESCs. Scale bar = 100 µm. (Right) Quantification of migrated cells per field. (C) qPCR analysis of mRNA expression levels for the EMT-related genes E-Cadherin, N-Cadherin, and β-Catenin in NRK-52E cells. (D) Western blot analysis of protein expression levels for the EMT markers Vimentin and β-Catenin in NRK-52E cells. (E) Representative immunofluorescence images of uterine tissue sections stained for E-Cadherin (red) and Vimentin (green). Nuclei were counterstained with Hoechst (blue). Scale bar = 500 µm. Data are presented as mean ± SEM. *$p < 0.05$, **$p < 0.01$, ***$p < 0.001$, ****$p < 0.0001$.

MAP3K7C1 and EGR2 mRNA expression was significantly downregulated ($p < 0.01$) (Fig. 6C,D).

3.6 hUCMSC-Exos Inhibit Cell Migration by Downregulating EGR2

To further elucidate the downstream targets of hUCMSC-exos, we performed Western blot analysis to as-

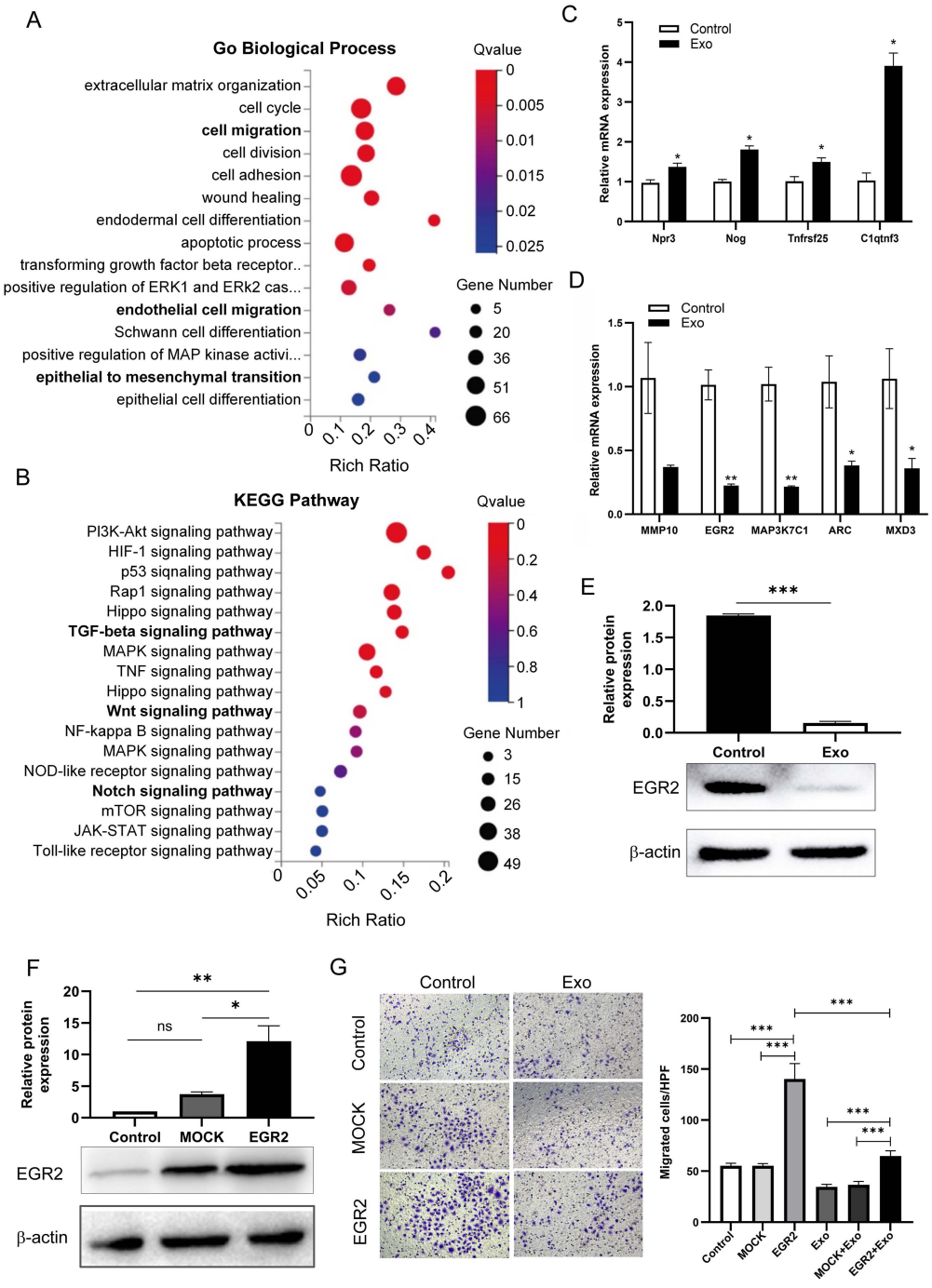

Fig. 6. Transcriptomic analysis and functional validation of EGR2 in hUCMSC- Exo-Mediated therapy. (A,B) Enrichment analysis of differentially expressed genes in primary rat endometrial cells after exosome treatment. (A) Gene Ontology (GO) terms and (B) Kyoto Encyclopedia of Genes and Genomes (KEGG) pathways were significantly enriched. (C,D) The mRNA expression of upregulated genes (C) and downregulated genes (D) in primary rat endometrial cells after exosome treatment. (E) EGR2 protein expression in NRK-52E cells after exosome treatment was detected by Western blot. (F) EGR2 protein expression in NRK-52E cells transfected with an EGR2 plasmid versus an empty vector was detected by Western blot. (G) (Left) Transwell migration assay (crystal violet staining) of NRK-52E cells overexpressing EGR2 or empty vector, with or without exosome treatment. (Right) Quantification of migrated cells. Scale bar = 100 μm. Data are presented as mean ± SEM. *$p < 0.05$, **$p < 0.01$, ***$p < 0.001$.

sess the protein levels of EGR2. The results revealed a significant decrease in EGR2 protein expression, which aligned with the transcriptome sequencing data, further confirming that hUCMSC-exos exert a negative regulatory effect on EGR2 expression (Fig. 6E). To investigate the role of EGR2 in cell migration, we overexpressed EGR2 in

rat renal epithelial cells using plasmid transfection technology. The Western blot results demonstrated a notable increase in EGR2 protein levels in the overexpression group (Fig. 6F). Transwell migration assays revealed a marked increase in the number of infiltrating cells in the EGR2-overexpressing group, indicating that EGR2 promotes cell migration. However, following exosome treatment, these pro-migration phenotypes were reversed. In conclusion, the findings of this study confirm that hUCMSC-exos can inhibit cell migration by downregulating EGR2 expression (Fig. 6G).

4. Discussion

This study demonstrated that a PF-127 thermosensitive hydrogel loaded with hUCMSC-exos effectively delivered and prolonged exosome retention in the injured uterus. By inhibiting the EMT process, the hydrogel significantly improved ethanol-induced endometrial damage in rats, promoted tissue morphological repair, reduced fibrosis, and partially restored fertility. The underlying molecular mechanism may be associated with the downregulation of the key transcription factor EGR2 by exosomes.

First, our results confirm the superiority of PF-127 hydrogel as an exosome delivery vehicle. The hydrogel undergoes rapid gelation at body temperature, achieving both localization and sustained exosome release (up to 12 days) at the injury site, while demonstrating excellent biocompatibility without eliciting significant foreign body reactions. These findings provide a viable strategy to overcome the application bottlenecks of the short *in vivo* half-life and poor targeting of exosomes, aligning with recent research trends that utilize biomaterials to enhance the delivery of cytokines or exosomes for improved tissue regeneration effects [25]. Previous studies have employed PF-127-loaded mesenchymal stem cells for intrauterine injection therapy in rat endometrial injury models [26,27]. Other studies have utilized collagen scaffolds or hyaluronic acid hydrogel (HA gel)-loaded MSC-exos to promote endometrial regeneration [28,29]. To our knowledge, this is the first study to adopt PF-127-loaded MSC-exos for intrauterine injection, achieving a notable sustained release effect. This prolonged retention is likely attributable to the *in situ* gelation administration route (liquid at room temperature, gelling at body temperature) and the precise injection directly into the endometrial injury site, which enhance local anchoring and reduce clearance.

In terms of therapeutic effects, PF-127-hUCMSC-exo treatment significantly increased endometrial thickness and the number of glands, reduced collagen deposition, and ultimately improved the embryo implantation rate in damaged uteri. These findings align with those of previous reports indicating that various sources of MSCs, including bone marrow MSCs (BMMSCs) [30], menstrual blood-derived MSCs (MenSCs) [31], umbilical cord-derived MSCs (UC-MSCs) [32], and adipose tissue-derived MSCs (AD-MSCs) [33], have potential efficacy in endometrial regeneration therapy. Furthermore, exosomes derived from BMMSCs can significantly increase the number of endometrial glands and markedly reduce the area of endometrial fibrosis. The underlying mechanism may involve the suppression of EMT through the activation of the Wnt/β-catenin signaling pathway [34,35]. A collagen scaffold structure loaded with UCMSC-exos promotes endometrial regeneration and restores fertility by inducing CD163+ M2 macrophage polarization [28]. These therapeutic actions are consistent with the emerging body of evidence highlighting the anti-inflammatory and antioxidant capacities of MSC-conditioned products [36]. In summary, MSCs and their exosomes primarily facilitate the repair of endometrial damage through mechanisms as promoting endometrial cell proliferation and regeneration, suppressing inflammation and fibrosis, and modulating immune responses.

This study further investigated the repair mechanism through the regulation of EMT. We found that hUCMSC-exos can upregulate the expression of the epithelial marker E-cadherin while downregulating the expression of the mesenchymal markers vimentin and β-catenin both *in vivo* and *in vitro*, thereby inhibiting the migration ability of endometrial cells. These findings strongly suggest that exosomes exert their antifibrotic effects by reversing or suppressing the abnormal EMT induced by injury. Transcriptomic analysis revealed that differentially expressed genes were significantly enriched in EMT- and related-pathway genes after exosome intervention. Studies have demonstrated that exosomal miR-466f-3p derived from mouse MSCs reverses the EMT process by inhibiting the AKT/GSK3β pathway via c-MET in radiation-induced lung injury [24]. Additionally, the delivery of lncRNA GAS5 by hUCMSC-exos alleviates EMT through competitive binding to miR-21, thereby restoring PTEN expression [37]. In an epithelial–mesenchymal transition cell model of the human peritoneal mesothelial cell line (HMrSV5), lnc-CDHR contained in hUCMSC-exos modulates the inhibition of the target gene PTEN by competitively binding to miR-3149, thus attenuating EMT in HMrSV5 through the AKT/FOXO pathway [38]. Therefore, we believe that the repair of endometrial injury by hUCMSC-exos is primarily associated with the inhibition of EMT progression. To this end, we further identified the enriched differentially expressed genes and validated EGR2 (early growth response 2) as a key downstream target of the effects of hUCMSC-exos.

EGR2 is a zinc finger transcription factor that belongs to the early growth response protein family. It is typically rapidly induced by growth factors, stress signals, or differentiation signals and participates in the regulation of various pathological processes, including inflammation, fibrosis, and cell migration [39,40]. EGR2 is significantly upregulated in fibrotic skin and lung tissues from systemic sclerosis patients. As a direct transcriptional target of TGF-β, its overexpression enhances collagen synthesis and myofibroblast differentiation [41]. The study on liver fibro-

sis revealed that reduced EGR2 expression could inhibit the transition from benign hepatic steatosis to liver fibrosis [42]. In renal fibrosis patient samples, EGR2 expression was increased. Overexpression of EGR2 promoted renal fibrosis in unilateral ureteral obstruction mice, while EGR2 gene deletion alleviated obstructive nephropathy and reduced the occurrence of EMT, which was associated with the p-STAT3-EGR2-p-Smad3 axis [43]. Studies have revealed that EGR2 can form a transcriptional complex with the histone acetyltransferase p300/CBP, increasing chromatin accessibility and activating the transcription of downstream target genes (such as SNAI2) [44]. This epigenetic regulatory mechanism is particularly critical during EMT, as SNAI2, a core EMT transcription factor, can directly suppress E-cadherin expression and activate mesenchymal markers such as vimentin [45]. Therefore, under pathological conditions such as chronic inflammation and cancer, EGR2 is often abnormally induced and acts as a driver of EMT, promoting invasion and fibrosis.

In this study, we demonstrated that MSC-derived exosomes effectively suppressed EGR2 expression in endometrial stromal cells. However, the specific exosomal cargo responsible for this regulation remained to be elucidated. Considering the well-established role of exosomal miRNAs in mediating post-transcriptional gene regulation, we performed a computational prediction using TargetScan (v8.0) to identify potential miRNAs that may target EGR2. This analysis revealed several high-confidence candidates, including miR-150-5p, miR-17-5p, miR-20a-5p, and miR-106b-5p. Notably, miR-150-5p and miR-17-5p have been previously reported to be enriched in MSC-derived exosomes and associated with anti-fibrotic functions [46,47]. Nevertheless, the precise mechanisms by which these miRNAs may regulate EGR2 in our model require further experimental validation, and this represents an important direction for future investigation.

5. Limitations

This study first shows that hUCMSC-exos suppress EGR2 expression, thereby inhibiting EMT and fibrosis and revealing new mechanistic insights into MSC-exos mediated endometrial epithelial homeostasis. However, this study has certain limitations. First, while PF-127 hydrogel enhances retention time, its specific *in vivo* degradation kinetics and long-term effects on the uterine cavity microenvironment require further detailed evaluation. In addition, our study did not include a direct head-to-head comparison between PF-127 loaded and free exosomes, and thus we are unable to quantify the exact fold-improvement over free exosomes. Second, the specific active components in exosomes (such as the particular miRNA or protein) responsible for downregulating EGR2 have not yet been identified, which represents a key direction for future functional research. Future research should focus on identifying the key functional molecules in exosomes responsible for therapeutic effects and optimizing the physicochemical properties of the hydrogel to advance this strategy toward clinical application. Moreover, our RNA-seq identified multiple candidate genes, but only EGR2 was functionally validated in the present study, and thorough characterization of the remaining DEGs is an important direction for future investigation. Finally, although the rat endometrial injury and repair model can simulate some pathological features of humans, there are differences in etiology and pathological progression compared with the complex intrauterine adhesions observed in humans. Therefore, clinical translation of the research findings should be approached with caution, the complementary models would be valuable for further validation.

6. Conclusions

This study demonstrates that a PF-127 thermosensitive hydrogel loaded with hUCMSC-exos serves as an effective delivery system, significantly prolonging exosome retention in the injured uterus. Intrauterine injection of PF-127-hUCMSC-exos markedly improved ethanol-induced endometrial damage in rats, as evidenced by increased endometrial thickness and gland number, reduced collagen deposition and fibrosis, and partially restored fertility. Mechanistically, the therapeutic effects are primarily attributed to inhibition of the EMT process, mediated by downregulation of the key transcription factor EGR2. To the best of our knowledge, we first identify EGR2 as a functional downstream target through which hUCMSC-exos drive endometrial repair following injury. While the PF-127 hydrogel offers excellent biocompatibility and sustained release, further evaluation of its long-term degradation kinetics and uterine microenvironment effects is warranted. Despite limitations inherent to the rat model, these findings provide a promising biomaterial-assisted exosome therapy for endometrial injury and offer new molecular insights into EMT-based antifibrotic mechanisms.

Disclosure

The paper is listed as, “PF-127 Hydrogel-Delivered hUCMSC-Exosomes Attenuate Endometrial Injury by Inhibiting Epithelial–Mesenchymal Transition” as a preprint on Research Square at: https://assets-eu.researchsquare.com/files/rs-9166394/v1/10411fbe-649b-46d1-a10d-013209d207fd.pdf?c=1776949000.

Availability of Data and Materials

All data reported in this paper will also be shared by the corresponding authors contact upon request.

Author Contributions

LB, LL, ST and YT performed the experiments; ZW, JT, HZ and RL analyzed the data; XZ and RL designed and conceived this study. LB, XZ and RL wrote the manuscript, LL obtained the funding. All authors contributed to edito-

rial changes in the manuscript. All authors read and approved the final manuscript. All authors have participated sufficiently in the work and agreed to be accountable for all aspects of the work.

Ethics Approval and Consent to Participate

The study was conducted in accordance with the AVMA Guidelines for the Euthanasia of Animals. The study was carried out in accordance with the ARRIVE guidelines. The research protocol was approved by the Ethics Committee of Hunan Normal University (permit number: 2022431; approval Date: October 2022).

Acknowledgment

We gratefully acknowledge Guang Zhao of Hunan Shengbao Biotechnology Co., Ltd. for providing human umbilical cord mesenchymal stem cell serum-free culture supernatant.

Funding

This study was supported by grants from the Hunan Provincial Health Commission Project (grant number B202302076420); Changsha Municipal Natural Science Foundation (grant number kq2403185); and the Natural Science Foundation of Hunan Province (grant number 2025JJ80509).

Conflicts of Interest

The authors declare no conflicts of interest. Shengbin Tang and Yezi Tang are employed by Hunan Shengbao Biotechnology Co., Ltd. The authors declare that this affiliation does not influence the study design, data collection, analysis, interpretation, or the decision to publish.

Supplementary Material

Supplementary material associated with this article can be found, in the online version, at https://doi.org/10.31083/FBL53953.

References

[1] Zhang J, Shi C, Sun J, Niu J. Analysis of factors affecting the prognosis of patients with intrauterine adhesions after transcervical resection of adhesions. Fertility and Sterility. 2024; 122: 365–372. https://doi.org/10.1016/j.fertnstert.2024.03.016

[2] Trinh TT, Nguyen KD, Pham HV, Ho TV, Nguyen HT, O'Leary S, et al. Effectiveness of Hyaluronic Acid Gel and Intrauterine Devices in Prevention of Intrauterine Adhesions after Hysteroscopic Adhesiolysis in Infertile Women. Journal of Minimally Invasive Gynecology. 2022; 29: 284–290. https://doi.org/10.1016/j.jmig.2021.08.010

[3] Xu P, Xu H, Lu Q, Ling S, Hu E, Song Y, et al. Reproductive outcomes following copper-containing intrauterine device after hysteroscopic lysis for intrauterine adhesions. Experimental and Therapeutic Medicine. 2024; 27: 175. https://doi.org/10.3892/etm.2024.12463

[4] Zhang D, Du Q, Li C, Ding C, Chen J, He Y, et al. Functionalized human umbilical cord mesenchymal stem cells and injectable HA/Gel hydrogel synergy in endometrial repair and fertility recovery. Acta Biomaterialia. 2023; 167: 205–218. https://doi.org/10.1016/j.actbio.2023.06.013

[5] Hou Z, Yang T, Xu D, Fu J, Tang H, Zhao J, et al. hUC-MSCs loaded collagen scaffold for refractory thin endometrium caused by Asherman syndrome: a double-blind randomized controlled trial. Stem Cells Translational Medicine. 2025; 14: szaf011. https://doi.org/10.1093/stcltm/szaf011

[6] Antonio-Ríos G, Ribas-Aparicio RM, Leyva-Gómez G, Soldevila G, Dueñas KAE, Trejo-Iriarte CG, et al. The Impact of Large-Scale Expansion on the Functional Properties of Mesenchymal Stem Cells. Stem Cell Reviews and Reports. 2026; 22: 1051–1066. https://doi.org/10.1007/s12015-026-11068-x

[7] Yu X, Shi L, Zhang Y, Wang H, Wang H. A Comparative Study of Mesenchymal Stem Cells from Various Sources in Endometrial Repair: the Significant Advantages of Decidual Mesenchymal Stem Cells. Stem Cell Reviews and Reports. 2025; 21: 2667–2670. https://doi.org/10.1007/s12015-025-10950-4

[8] Zhou Y, Li Q, You S, Jiang H, Jiang L, He F. Efficacy of Mesenchymal Stem Cell-Derived Extracellular Vesicles in the Animal Model of Female Reproductive Diseases: A Meta-Analysis1. Stem Cell Reviews and Reports. 2023; 19: 2299–2310. https://doi.org/10.1007/s12015-023-10576-4

[9] Zeng X, Liao Y, Huang D, Yang J, Dai Z, Chen Z, et al. Exosomes derived from hUC-MSCs exhibit ameliorative efficacy upon previous cesarean scar defect via orchestrating β-TrCP/CHK1 axis. Scientific Reports. 2025; 15: 489. https://doi.org/10.1038/s41598-024-84689-2

[10] Megha KB, Swathi S, Joseph X, Vandana U, Mohanan PV. Cytocompatibility of Pluronics F-127 on adenocarcinomic human alveolar basal epithelial cells (A549 cells). Environmental Science and Pollution Research International. 2022; 29: 71124–71135. https://doi.org/10.1007/s11356-022-20925-4

[11] Li S, Yang C, Li J, Zhang C, Zhu L, Song Y, et al. Progress in Pluronic F127 Derivatives for Application in Wound Healing and Repair. International Journal of Nanomedicine. 2023; 18: 4485–4505. https://doi.org/10.2147/IJN.S418534

[12] Yang J, Chen Z, Pan D, Li H, Shen J. Umbilical Cord-Derived Mesenchymal Stem Cell-Derived Exosomes Combined Pluronic F127 Hydrogel Promote Chronic Diabetic Wound Healing and Complete Skin Regeneration. International Journal of Nanomedicine. 2020; 15: 5911–5926. https://doi.org/10.2147/IJN.S249129

[13] Zhang Q, Su P, Zhao F, Ren H, He C, Wu Q, et al. Enhancing Skin Injury Repair: Combined Application of PF-127 Hydrogel and hADSC-Exos Containing miR-148a-3p. ACS Biomaterials Science & Engineering. 2024; 10: 2235–2250. https://doi.org/10.1021/acsbiomaterials.3c01567

[14] Kishta MS, Hafez AM, Hydara T, Hamed Z, Bahr MM, Shamaa AA, et al. The transforming role of wharton's jelly mesenchymal stem cell-derived exosomes for diabetic foot ulcer healing: a randomized controlled clinical trial. Stem Cell Research & Therapy. 2025; 16: 559. https://doi.org/10.1186/s13287-025-04690-y

[15] Jayachandran J, Srinivasan H, Mani KP. Molecular mechanism involved in epithelial to mesenchymal transition. Archives of Biochemistry and Biophysics. 2021; 710: 108984. https://doi.org/10.1016/j.abb.2021.108984

[16] Miyazawa K, Miyazono K. Regulation of TGF-β Family Signaling by Inhibitory Smads. Cold Spring Harbor Perspectives in Biology. 2017; 9: a022095. https://doi.org/10.1101/cshperspect.a022095

[17] Li J, Wang W, Li S, Qiao Z, Jiang H, Chang X, et al. Smad2/3/4 complex could undergo liquid liquid phase separation and induce apoptosis through TAT in hepatocellular carcinoma. Cancer Cell International. 2024; 24: 176. https://doi.org/10.1186/s12935-024-03353-x

[18] Bourdon M, Santulli P, Doridot L, Jeljeli M, Chêne C, Chouzenoux S, et al. Immune cells and Notch1 signaling appear to drive the epithelial to mesenchymal transition in the development of adenomyosis in mice. Molecular Human Reproduction. 2021; 27: gaab053. https://doi.org/10.1093/molehr/gaab053
[19] Wang X, Zhou J, Li X, Liu C, Liu L, Cui H. The Role of Macrophages in Lung Fibrosis and the Signaling Pathway. Cell Biochemistry and Biophysics. 2024; 82: 479–488. https://doi.org/10.1007/s12013-024-01253-5
[20] Rim EY, Clevers H, Nusse R. The Wnt Pathway: From Signaling Mechanisms to Synthetic Modulators. Annual Review of Biochemistry. 2022; 91: 571–598. https://doi.org/10.1146/annurev-biochem-040320-103615
[21] Schunk SJ, Floege J, Fliser D, Speer T. WNT-β-catenin signalling - a versatile player in kidney injury and repair. Nature Reviews. Nephrology. 2021; 17: 172–184. https://doi.org/10.1038/s41581-020-00343-w
[22] Wei J, Zhao Q, Yang G, Huang R, Li C, Qi Y, et al. Mesenchymal stem cells ameliorate silica-induced pulmonary fibrosis by inhibition of inflammation and epithelial-mesenchymal transition. Journal of Cellular and Molecular Medicine. 2021; 25: 6417–6428. https://doi.org/10.1111/jcmm.16621
[23] Xiao K, He W, Guan W, Hou F, Yan P, Xu J, et al. Mesenchymal stem cells reverse EMT process through blocking the activation of NF-κB and Hedgehog pathways in LPS-induced acute lung injury. Cell Death & Disease. 2020; 11: 863. https://doi.org/10.1038/s41419-020-03034-3
[24] Li Y, Shen Z, Jiang X, Wang Y, Yang Z, Mao Y, et al. Mouse mesenchymal stem cell-derived exosomal miR-466f-3p reverses EMT process through inhibiting AKT/GSK3β pathway via c-MET in radiation-induced lung injury. Journal of Experimental & Clinical Cancer Research : CR. 2022; 41: 128. https://doi.org/10.1186/s13046-022-02351-z
[25] He L, Li Q. Application of biomaterials in mesenchymal stem cell based endometrial reconstruction: current status and challenges. Frontiers in Bioengineering and Biotechnology. 2025; 13: 1518398. https://doi.org/10.3389/fbioe.2025.1518398
[26] Yang H, Wu S, Feng R, Huang J, Liu L, Liu F, et al. Vitamin C plus hydrogel facilitates bone marrow stromal cell-mediated endometrium regeneration in rats. Stem Cell Research & Therapy. 2017; 8: 267. https://doi.org/10.1186/s13287-017-0718-8
[27] Hu Q, Xie N, Liao K, Huang J, Yang Q, Zhou Y, et al. An injectable thermosensitive Pluronic F127/hyaluronic acid hydrogel loaded with human umbilical cord mesenchymal stem cells and asiaticoside microspheres for uterine scar repair. International Journal of Biological Macromolecules. 2022; 219: 96–108. https://doi.org/10.1016/j.ijbiomac.2022.07.161
[28] Xin L, Lin X, Zhou F, Li C, Wang X, Yu H, et al. A scaffold laden with mesenchymal stem cell-derived exosomes for promoting endometrium regeneration and fertility restoration through macrophage immunomodulation. Acta Biomaterialia. 2020; 113: 252–266. https://doi.org/10.1016/j.actbio.2020.06.029
[29] Zhang S, Wang D, Yang F, Shen Y, Li D, Deng X. Intrauterine Injection of Umbilical Cord Mesenchymal Stem Cell Exosome Gel Significantly Improves the Pregnancy Rate in Thin Endometrium Rats. Cell Transplantation. 2022; 31: 9636897221133345. https://doi.org/10.1177/09636897221133345
[30] Gao L, Huang Z, Lin H, Tian Y, Li P, Lin S. Bone Marrow Mesenchymal Stem Cells (BMSCs) Restore Functional Endometrium in the Rat Model for Severe Asherman Syndrome. Reproductive Sciences (Thousand Oaks, Calif.). 2019; 26: 436–444. https://doi.org/10.1177/1933719118799201
[31] Luo B, Zeng X, Luo L. Intrauterine adhesions repair with menstrual blood-derived mesenchymal stem cells via CXCL13-CXCR5 signal axis and its mechanism. Stem Cell Research & Therapy. 2024; 15: 380. https://doi.org/10.1186/s13287-024-03996-7
[32] Zhang L, Li Y, Dong YC, Guan CY, Tian S, Lv XD, et al. Transplantation of umbilical cord-derived mesenchymal stem cells promotes the recovery of thin endometrium in rats. Scientific Reports. 2022; 12: 412. https://doi.org/10.1038/s41598-021-04454-7
[33] Dai Y, Xin L, Hu S, Xu S, Huang D, Jin X, et al. A construct of adipose-derived mesenchymal stem cells-laden collagen scaffold for fertility restoration by inhibiting fibrosis in a rat model of endometrial injury. Regenerative Biomaterials. 2023; 10: rbad080. https://doi.org/10.1093/rb/rbad080
[34] Yao Y, Chen R, Wang G, Zhang Y, Liu F. Exosomes derived from mesenchymal stem cells reverse EMT via TGF-β1/Smad pathway and promote repair of damaged endometrium. Stem Cell Research & Therapy. 2019; 10: 225. https://doi.org/10.1186/s13287-019-1332-8
[35] Yuan L, Cao J, Hu M, Xu D, Li Y, Zhao S, et al. Bone marrow mesenchymal stem cells combined with estrogen synergistically promote endometrial regeneration and reverse EMT via Wnt/β-catenin signaling pathway. Reproductive Biology and Endocrinology : RB&E. 2022; 20: 121. https://doi.org/10.1186/s12958-022-00988-1
[36] Abd-Rabou AA, Youssef AM, El-Khonezy MI, Kotob SE, Kishta MS. Anti-Inflammatory/Antioxidant Features of Adipose Tissue Mesenchymal Stem Cells Conditioned Media for Doped TiO_2 Nanoparticles in Induced Inflammation. ChemistryOpen. 2025; 14: e202500261. https://doi.org/10.1002/open.202500261
[37] Huang Y, Ma J, Fan Y, Yang L. Mechanisms of human umbilical cord mesenchymal stem cells-derived exosomal lncRNA GAS5 in alleviating EMT of HPMCs via Wnt/β-catenin signaling pathway. Aging. 2023; 15: 4144–4158. https://doi.org/10.18632/aging.204719
[38] Jiao T, Huang Y, Sun H, Yang L. Exosomal lnc-CDHR derived from human umbilical cord mesenchymal stem cells attenuates peritoneal epithelial-mesenchymal transition through AKT/FOXO pathway. Aging. 2023; 15: 6921–6932. https://doi.org/10.18632/aging.204883
[39] Bo Z, Huang S, Li L, Chen L, Chen P, Luo X, et al. EGR2 is a hub-gene in myocardial infarction and aggravates inflammation and apoptosis in hypoxia-induced cardiomyocytes. BMC Cardiovascular Disorders. 2022; 22: 373. https://doi.org/10.1186/s12872-022-02814-3
[40] Hou X, Hu G, Wang H, Yang Y, Sun Q, Bai X. Inhibition of Egr2 Protects against TAC-induced Heart Failure in Mice by Suppressing Inflammation and Apoptosis Via Targeting Acot1 in Cardiomyocytes. Journal of Cardiovascular Translational Research. 2025; 18: 574–585. https://doi.org/10.1007/s12265-025-10602-5
[41] Fang F, Ooka K, Bhattacharyya S, Wei J, Wu M, Du P, et al. The early growth response gene Egr2 (Alias Krox20) is a novel transcriptional target of transforming growth factor-β that is up-regulated in systemic sclerosis and mediates profibrotic responses. The American Journal of Pathology. 2011; 178: 2077–2090. https://doi.org/10.1016/j.ajpath.2011.01.035
[42] Iwata A, Maruyama J, Natsuki S, Nishiyama A, Tamura T, Tanaka M, et al. Egr2 drives the differentiation of $Ly6C^{hi}$ monocytes into fibrosis-promoting macrophages in metabolic dysfunction-associated steatohepatitis in mice. Communications Biology. 2024; 7: 681. https://doi.org/10.1038/s42003-024-06357-5
[43] Song A, Yan R, Xiong W, Xiang H, Huang J, Jiang A, et al. Early growth response protein 2 promotes partial epithelial-mesenchymal transition by phosphorylating Smad3 during renal fibrosis. Translational Research : the Journal of Laboratory and Clinical Medicine. 2024; 271: 13–25. https://doi.org/10.1016/j.

trsl.2024.04.005
[44] Noritsugu K, Ito A, Nakao Y, Yoshida M. Identification of zinc finger transcription factor EGR2 as a novel acetylated protein. Biochemical and Biophysical Research Communications. 2017; 489: 455–459. https://doi.org/10.1016/j.bbrc.2017.05.170
[45] Mohammad SI, Vasudevan A, Nadhim Mohammed S, Uthirapathy S, M M R, Kundlas M, et al. Anti-metastatic potential of flavonoids for the treatment of cancers: focus on epithelial-mesenchymal transition (EMT) process. Naunyn-Schmiedeberg's Archives of Pharmacology. 2025; 398: 14849–14875. https://doi.org/10.1007/s00210-025-04235-3
[46] Du Z, Wu T, Liu L, Luo B, Wei C. Extracellular vesicles-derived miR-150-5p secreted by adipose-derived mesenchymal stem cells inhibits CXCL1 expression to attenuate hepatic fibrosis. Journal of Cellular and Molecular Medicine. 2021; 25: 701–715. https://doi.org/10.1111/jcmm.16119
[47] Tian Y, Jin M, Ye N, Gao Z, Jiang Y, Yan S. Mesenchymal stem cells-derived exosomes attenuate mouse non-heart-beating liver transplantation through Mir-17-5p-regulated Kupffer cell pyroptosis. Stem Cell Research & Therapy. 2025; 16: 57. https://doi.org/10.1186/s13287-025-04169-w